A CAD LABORATORY IN ELECTROMAGNETICS FOR UNDERGRADUATES

R. Mertens, A. Peytier, K. Hameyer and R. Belmans

Katholieke Universiteit Leuven, Belgium

Abstract. The CAD laboratory gives the students an idea when to use the different approaches to deal with magnetic circuits. They start with a simplified analytical model and are then confronted with the finite element method, even in three dimensions. Calculations and measurements are compared and discussed.

Keywords. education, laboratory, magnetic circuits

A CAD LAB AT THE DEPARTMENT OF ELECTRICAL ENGINEERING

After two years of education in basic engineering sciences, students of the third year of their master's degree are confronted with technical courses. An educational complement for the course "General Electricity, Electrical Machines and Drives - part 1" is a CAD laboratory in electromagnetics. In this laboratory, the analysis of different electromagnetic objects used in power electronic converters and variable speed drives is given. Limitations of classical approaches and comparison with measurements are provided. In spite of its rather simple construction, a core of laminated iron and a coil of copper (fig. 1), an E-core inductor has a lot to offer as a subject of a CAD lab. After all, inductors are used in all kind of converters as commutating and smoothing inductors, as part of protective circuits and filters, or just as an impedance. It has to be realised that passive components (inductors and capacitors) represent 1/3 of all the cost of power electronic converter (1). The aim of this CAD lab is that students compare the different methods and their restrictions, for calculating the inductance. A commercial finite element program on UNIX-workstations, a spreadsheet program on PCs and the standard measuring equipment of a electrical machine laboratory are available for this purpose.

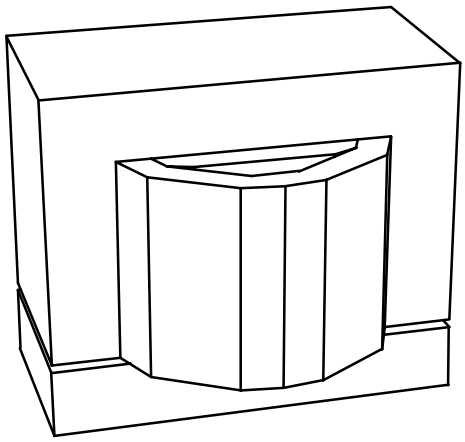

Figure 1: Three dimensional view of the E-core inductor

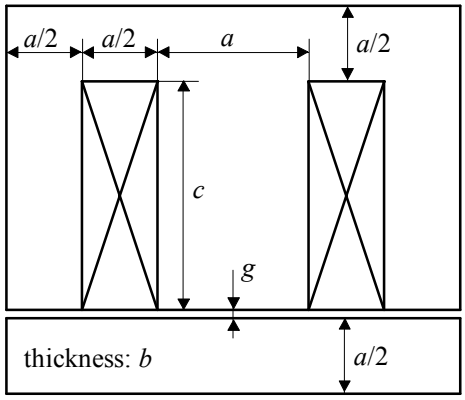

Figure 2: Cross section and dimensions of the E-core inductor

CONTENTS OF THE CAD LAB

Magnetic circuit approach

Air gap reluctances. A magnetic circuit (Hopkinson's law, comparable to Ohm's law for electric circuit) is a first approach to calculate the outer inductance. The magnetic circuit is described by a flux tube model. The flux tubes are represented by their reluctances.

TABLE 1 - Rated values and dimensions of the E-core inductor

L = 150 mH	g = 3.3 mm
I = 10 A	a = 6 cm
N = 288	b = 9 cm
	c = 9 cm

A first approximation is obtained by neglecting the magnetomotive force (*MMF*) in the iron and the leakage flux. The inductance L can be found by first calculating the total reluctance $\Re_m$ and evaluating

$$L = \frac{N^2}{\Re_m} , \tag{1}$$

where N is the number of turns of the coil.

To take the fringing effect into consideration, correction factors for the cross-section of the air gap S_1 beneath the centre leg of the E-core with length g, are used.

$$S_1 = (a + 1...2\,g)(b + 1...2\,g) , \tag{2}$$

where a and b are the dimensions of the core cross-section.

Two different air gap reluctances can be found in the inductor. $\Re_{m1}$ is the reluctance of the air gap beneath the centre leg and $\Re_{m2}$ is the reluctance of the air gap beneath the right or left leg. The total reluctance is given by

$$\Re_m = \Re_{m1} + \frac{\Re_{m2}}{2} , \tag{3}$$

with

$$\Re_{m1} = \frac{g}{\mu_0 (a + 1...2\,g)(b + 1...2\,g)} \tag{4}$$

$$\Re_{m2} = \frac{g}{\mu_0 \left(\frac{a}{2} + 1...2\,g\right)(b + 1...2\,g)} . \tag{5}$$

Table 1 and fig. 2 show the dimensions of the inductor used in the CAD laboratory. Table 2 shows the results of the analytical inductance calculation.

Superposing of flux-*MMF* plots. The second approach includes the non-linearity of the iron parts by superposing the flux-*MMF* plot of the air gap with the flux-*MMF* plot of the iron parts.

Table 3 shows the working scheme for this method. Two different magnetic flux tubes can be distinguished, the magnetic flux Φ_1 in the centre leg of the E-core and the magnetic flux Φ_2 in the right or the left leg. Therefore, the two different paths are handled separately. Starting from the magnetisation curve of the iron (step 1), shown in fig. 3, a flux-*MMF* plot (step 2) is constructed.

TABLE 2 - Inductance by calculating the air gap reluctances

Correction factor caused by fringing effects: 1 g	
$\Re_{m1}$ = 4.447 10^5 H^{-1}	
$\Re_{m2}$ = 8.452 10^5 H^{-1}	
L = 0.096 H	
Correction factor caused by fringing effects: 2 g	
$\Re_{m1}$ = 4.082 10^5 H^{-1}	
$\Re_{m2}$ = 7.428 10^5 H^{-1}	
L = 0.106 H	

TABLE 3 - Working scheme for the superposing of flux-*MMF* plots

Step 1	H	$\Rightarrow$	B
Step 2	$MMF = H\,\ell$	$\Rightarrow$	$\Phi = B\,S$
Step 3	MMF	$\Rightarrow$	$\Phi = \frac{MMF}{\Re_m}$
Step 4	MMF	$\Rightarrow$	Φ
Step 5	$I = \frac{MMF}{N}$	$\Rightarrow$	$L = \frac{N\,\Phi}{I}$

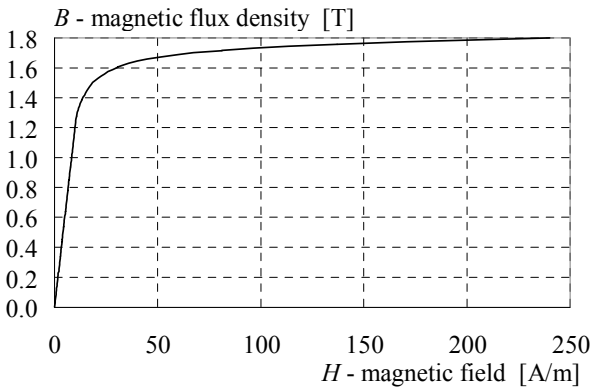

Figure 3: Non-linear magnetisation curve of the iron parts

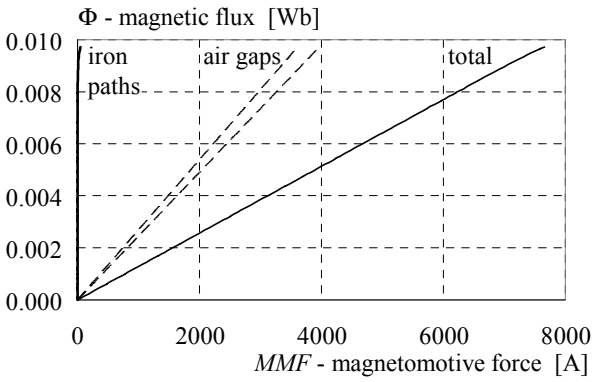

Figure 4: Total and partial flux-*MMF* plots

The average length of a flux line for the two different paths is given by

$$\ell_1 = a + c \tag{6}$$

$$\ell_2 = 2a + c \ . \tag{7}$$

The flux-*MMF* plot for the air gap (step 3) is defined by the reluctance. Therefore, the fringing effects are included. The relation between the two different flux tubes defines how the students have to combine the flux-*MMF* plots (step 4).

$$\Phi_2 = \frac{\Phi_1}{2} \tag{8}$$

Fig. 4 shows the total flux-*MMF* plot. The dashed lines are the flux-*MMF* plots of the two air gaps. The lines near the Φ-axis are the flux-*MMF* plots of the iron paths.

In the last step, the inductance as a function of the current is obtained (fig. 5). Table 4 gives the result for the inductance for the rated value of the current.

Finite element method in two dimensions

CARTER factor of a slot. As a second method for the field calculation, the students use the finite element method. To become familiar with the CAD software, the CARTER factor of a slot (fig. 6), is calculated and compared with the analytical result.

The CARTER factor is defined as the ratio of two air gap lengths, the real length g of the air gap and the equivalent length δ of a smooth air gap (without slots) in which the same magnetic energy is stored.

$$k_c = \frac{\delta}{g} \tag{9}$$

The CARTER factor is defined in (10)

$$k_c = \frac{\lambda}{\lambda - \alpha g} \ , \tag{10}$$

with

$$\alpha = \frac{4}{\pi}\left(\beta \arctan(\beta) - \ln\sqrt{1+\beta^2}\right) \tag{11}$$

$$\beta = \frac{w}{2g} \tag{12}$$

slot width: $w = \frac{a}{2}$ (13)

slot pitch: $\lambda = \frac{3a}{2}$. (14)

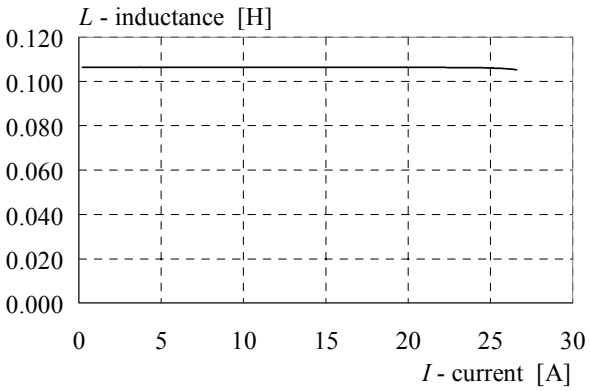

Figure 5: Calculation of the inductance by superposing the flux-*MMF* plots

TABLE 4 - Calculation of the inductance by superposing the flux-*MMF* plots

Correction factor caused by fringing effects: 1 *g*

L = 0.096 H (I = 10 A)

Correction factor caused by fringing effects: 2 *g*

L = 0.106 H (I = 10 A)

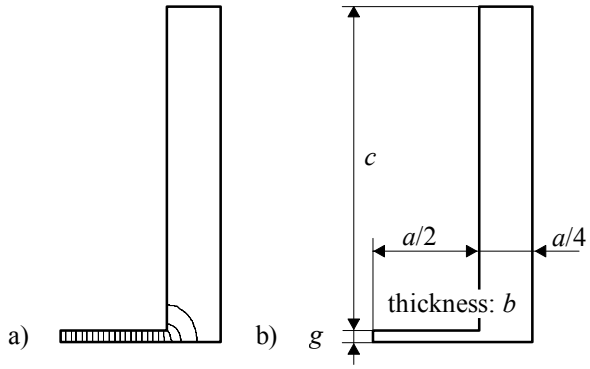

Figure 6: a) Flux density distribution (FEM) and b) dimensions of the slot for CARTER factor determination

TABLE 5 - Calculation of the Carter factor of a slot

Analytical result:

k_c = 1.27

Finite element calculation:

k_c = 1.28

with:

Φ = 0.09 Wb

W = 3.357 10^3 J

δ = 4.2 mm

The equivalent length of the air gap is calculated by the finite element method as

$$\delta = \frac{2\mu_0 S W}{\Phi^2} \ , \tag{15}$$

with

$$\Phi = \left(A_{left} - A_{right} \right) b$$

$$S = \frac{3a}{4} b \ . \tag{16}$$

The magnetic flux Φ is forced by applying the correct values for the magnetic vectorpotential A at the left and the right side of half the air gap. S is the cross-section of the air gap in the finite element model according to fig. 6. W is the magnetostatic energy stored in the finite element model and calculated with the post-processor of the FE-program as

$$W = \int \frac{1}{2\mu} B^2 \, \mathrm{d}V \ . \tag{17}$$

Table 5 shows the result for the Carter factor.

Inductance calculation. The calculation of the inductance is based on the identification of the magnetic energy W stored in the inductor expressed in magnetic quantities

$$W = \int \left(\int H \, \mathrm{d}\, B \right) \mathrm{d}V \ , \tag{18}$$

and the same energy expressed in electric quantities

$$W = \frac{1}{2} L I^2 \ , \tag{19}$$

where I is the current.

Figure 7 shows a flux plot of the finite element solution of the inductor, while table 6 shows the result of the finite element calculation of the inductance. For comparison, a two dimensional approximation (neglecting fringing effects in the third dimension) is done by calculating the air gap reluctances.

Improvement of the magnetic circuit

If the students have to compare the results of both approaches, they notice a difference due to the fact that the leakage flux is neglected and the fringing effect is underestimated in the magnetic circuit.

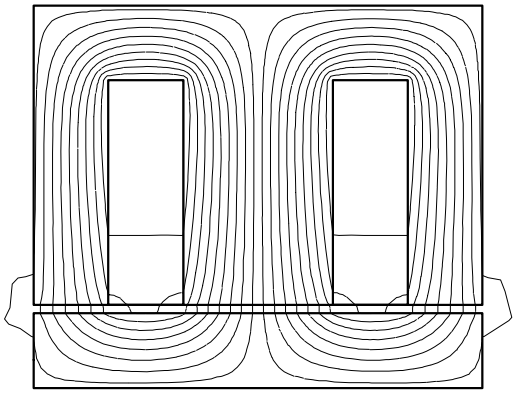

Figure 7: Flux plot of the inductor

TABLE 6 - Two dimensional finite element calculation of the inductance

Finite element solution:

$W = 5.94$ J
$L = 0.119$ H

Calculation of the air gap reluctances:
(correction factor caused by fringing effects: 2 g)

$\Re_{m1} = 4.381\ 10^5$ H^{-1}
$\Re_{m2} = 7.972\ 10^5$ H^{-1}
$L = 0.099$ H

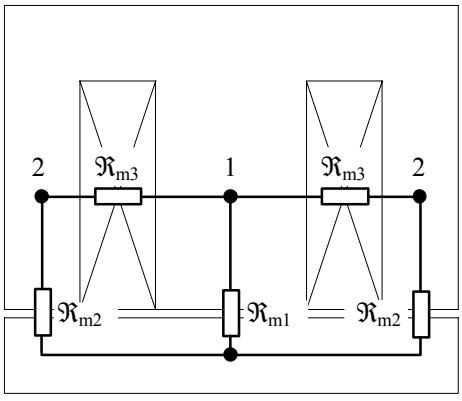

Figure 8: Improved magnetic circuit of the inductor

TABLE 7 - Calculation of the inductance with the improved magnetic circuit

$k_f = 1.61$
$\Re_{m1} = 4.133\ 10^5$ H^{-1}
$\Re_{m2} = 7.897\ 10^5$ H^{-1}
$\Re_{m3} = 8.842\ 10^6$ H^{-1}
$\Re_m = 6.833\ 10^5$ H^{-1}
$L = 0.121$ H

The finite element method inherently considers these mentioned effects. To improve the first approach, the students can see the E-core as two slots of the stator of an induction machine with a smooth rotor. Based on the CARTER factor, slot reluctance and leakage reactance calculations of induction machines, the students can obtain a more accurate approximation of the equivalent cross-section of the air gap.

A first possibility is to include the leakage flux by calculating the reluctance of the slot in which the current is flowing. This reluctance $\Re_{m3}$ is given by

$$\Re_{m3} = 3\frac{a/2}{\mu_0 b c} \quad . \tag{20}$$

The total reluctance (fig. 8) is given by

$$\frac{1}{\Re_m} = \frac{1}{\Re_{m1} + \frac{\Re_{m2}}{2}} + \frac{1}{\frac{\Re_{m3}}{2}} \quad . \tag{21}$$

A second possibility is to base the correction due to fringing on the CARTER factor. The same air gap can be seen in two different ways, but with the same reluctance.

$$\frac{k_c\, g}{\mu_0\, \lambda b} = \frac{g}{\mu_0 \left(\lambda - w + 2 k_f\, g\right) b} \tag{22}$$

This correction factor k_f is given by

$$k_f = \beta - \frac{\alpha}{2} \quad . \tag{23}$$

The cross-section S_1 of the air gap beneath the centre leg of the E-core is given by (neglecting fringing in the third dimension)

$$S_1 = \left(a + 2 k_f\, g\right) b \quad . \tag{24}$$

For the cross-section S_2 of the air gap beneath the left or right leg, a combined correction is used. The correction based on the CARTER factor can only be used for the interior sides of the air gap. For the exterior sides, a correction of 0.5 g is used.

$$S_2 = \left(\frac{a}{2} + \left(0.5 + k_f\right) g\right) b \tag{25}$$

Table 7 shows the result for the inductance.

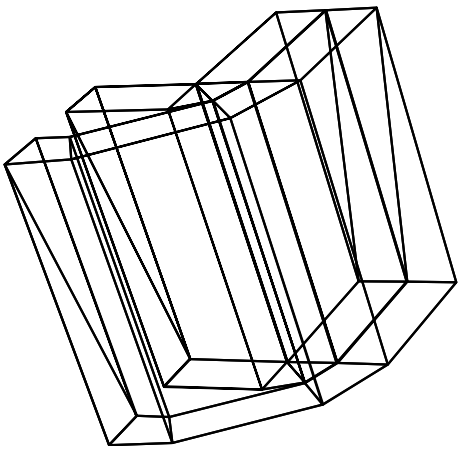

Figure 9: Finite element model of the two separate layers of the coil

TABLE 8 - Three dimensional finite element calculation of the inductance

k_s = 0.95
W (quarter model) = 2.001 J
W = 8.002 J
L = 0.160 H

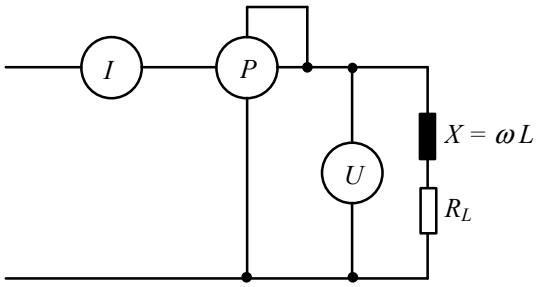

Figure 10: Electric circuit to measure the inductance

TABLE 9 - Calculation of the inductance using measured data

Measurements:
U = 461 V
I = 10.04 A
P = 97 W
Calculation:
f = 50 Hz
X = 45.91 Ω
L = 0.146 H

Finite element method in three dimensions

The influence of the length of the device is taken into account by using the finite element method in three dimensions. In this third approach modelling of the coil in two separate layers as shown in fig. 9, becomes possible. Based on symmetries only one quarter of the inductor has to be modelled. To reduce the computing time, the iron is assumed to be linear.

To give the students an idea how lamination can be modelled, they use an anisotropic material for the laminated iron core and calculate the equivalent relative permeability for the different directions:

$$\mu_{r\,X,Y} \approx k_s\, \mu_{r\,iron} \tag{26}$$

$$\mu_{r\,Z} \approx \frac{1}{1-k_s}\ , \tag{27}$$

where k_s is the stacking factor of the laminated core.

Table 8 gives the result of the three dimensional finite element calculation of the inductance.

Measurements

The inductance is measured by applying a sinusoidal voltage U (fig. 10). The current I is set to the rated value and the dissipated power P is measured. Table 9 shows the calculation of the inductance out of the measurements.

CONCLUSIONS

All electric machines have rated values and therefore the rated value for the inductance of the E-core inductor is compared with the results of the calculations and with measurements. This comparison gives the students an idea when to use an magnetic circuit approach (Hopkinson's law), or when they have to build a two or three dimensional finite element model. If the leakage flux can be neglected and they have knowledge of the fringing effect, they may use a simplified analytical approach. If the device can not be considered as infinitely long in the magnetic field calculations, they have to build a three dimensional finite element model. This understanding forms the basic of further CAD work with more difficult systems (permanent magnet motors, reluctance motors, induction motors, electromagnetic fields around power devices, etc.).

Acknowledgement

The authors are grateful to the Belgian Nationaal Fonds voor Wetenschappelijk Onderzoek for its financial support of this work and the Belgian Ministry of Scientific Research for granting the IUAP No. 51 on Magnetic Fields.

References

1. Thorborg, K., 1993, "Power Electronics in Theory and Practice", Studentlitteratur, Chartwell-Bratt.

2. de Jong, H. C. J., Lipo, T. A., Novtny, D. and Richter, E., August 23-25, 1993, "AC Machine Design", University of Wisconsin-Madison, College of Engineering.

3. Binns, K. J., Lawrenson, P. J. and Trowbridge, C. W., 1992, "The Analytical and Numerical Solutions of Electric and Magnetic Fields", John Wiley & Sons.

4. Silvester, P. P. and Ferrari, R. L., 1990, "Finite elements for Electrical Engineers", Cambridge University Press.

5. Lowther, D. A. and Silvester, P. P., 1986, "Computer-Aided Design in Magnetics", Springer-Verlag.

6. Kraus, J. D. and Carver, K. R., 1973, "Electromagnetics Second Edition", McGraw-Hill.

7. Richter, R., 1967, "Elektrische Maschinen Erster Band", Birkhäuser-Verlag.

8. Nürnberg, W., 1963, "Die Asynchronmaschine", Springer-Verlag.

9. Richter, R., 1963, "Elektrische Maschinen Zweiter Band", Birkhäuser-Verlag.

10. Carter, F. W., 1900, JIEE, 29, p. 925.

Address of the authors

Katholieke Universiteit Leuven
Dept. E. E., Div. ESAT / ELEN
Kardinaal Mercierlaan 94
B-3001 Leuven (Heverlee)
Belgium
Tel.: +32 16 321020
Fax: +32 16 321985